January 1980 LRP 162/80

THE TCA TOKAMAK

PROJECT REPORT 1979

A.D. Cheetham, A. Heym, F. Hofmann, K. Hruska,
R. Keller, A. Lietti, J.B. Lister, A. Pochelon,
H. Ripper, R. Schreiber, A. Simik

THE TCA TOKAMAK

PROJECT REPORT 1979

A.D. Cheetham, A. Heym, F. Hofmann, K. Hruska,
R. Keller, A. Lietti, J.B. Lister, A. Pochelon,
H. Ripper, R. Schreiber, A. Simik

Centre de Recherches en Physique des Plasmas
Association Euratom - Confédération Suisse
Ecole Polytechnique Fédérale de Lausanne

CH-1007 Lausanne / Switzerland

TABLE OF CONTENTS

1. Objectives

The main objective of the TCA Tokamak is to investigate the possibility of plasma heating by dissipation of Alfvén waves.

As is well known, additional heating is necessary to obtain ignition in a reactor based on the Tokamak concept. Many methods have been proposed and tested, mainly r.f. heating {1,2,3,4} at a wide range of frequencies and neutral beam heating {5,6}. None of these techniques gives entire satisfaction, although neutral beam heating is the method which has given the best results up to now {7,8}. It is however, expensive and inefficient at the beam energies required for a reactor. It is therefore necessary to test new methods. One of these is heating via the dissipation of Alfvén waves, which seems promising although it has not yet been tested on a Tokamak. The CRPP has been working for some years on this heating method and the work on a small linear pinch has demonstrated the excellent coupling betwen the r.f. generator and the plasma {9,10}. We now have to apply these results to a Tokamak and demonstrate the feasibility of this method.

For these reasons, the CRPP has undertaken the construction of a Tokamak, the TCA, (Tokamak, Chauffage Alfvén) of which the main aims are :
(1) Construction of a Tokamak of which the parameters are sufficient for the heating experiment. (2) Excitation of Alfvén waves in the plasma and the study of the optimum mode for heating together with the necessary antenna structure. (3) Study of the absorption mechanisms of large amplitude Alfvén waves with their effect on plasma stability and plasma transport.

The advantages of this project extend beyond this heating study in that it will make available to physicists in the CRPP and other Swiss universities a high temperature plasma for various studies, e.g. : (1) The CRPP

laser group is already preparing a collective scattering experiment for the Tokamak plasma, using a Far Infra Red laser beam. (2) A project to map the poloidal magnetic field using a heavy ion beam is under study. (3) Professor H. Schneider of Fribourg University is collaborating with the Tokamak Group by making bolometric measurements on the plasma. (4) Dr. S. Veprek of the Inorganic Chemistry Institute at the University of Zurich has submitted a research project concerning the plasma - wall interaction in the TCA Tokamak. A photograph and schematic of TCA are shown in Figs. 1 and 2.

In the long term the TCA may be updated to a non-circular cross-section Tokamak in which the plasma shape can be varied. In this form it would permit the study of the stability limits of these various configurations under high beta conditions produced by Alfvén heating, if successful. This part of the project could particularly interest Euratom since the cross-section could be made similar to that of JET. Other foreseeable phase II projects include ICRH studies.

2. Alfvén Wave Heating

The principle of the absorption of torsional Alfvén waves is well understood in the case of a cylindrical plasma {10,11,12,13,14}. The mechanism is the following :

When the plasma column is perturbed by an exterior magnetic field of defined frequency and wavelength, a torsional Alfvén wave is excited. At the location within the plasma where the phase velocity coincides with the Alfvén velocity, the wave amplitude is amplified by a resonance effect. The radius at which this takes place is determined by the plasma density and the confining field. The induced currents in the resonant layer saturate when the dissipation is equal to the power injected. This heating method allows us to deposit energy in the plasma interior in a

layer the position and thickness of which depend on the plasma parameters and the exciting wave parameters.

In linear geometry (e.g. screw pinch) the easiest mode to excite by external coils is the m = 1 mode. The plasma column experiences a helical deformation expressed as

$$\xi = \xi_o e^{i(m\theta - n\phi - \omega t)}$$

where θ is the angle around the axis and ϕ is the longitudinal coordinate. The real part of this expression represents the actual displacement, viz.

$$\xi_{real} = \xi_o \cos(m\theta - n\phi - \omega t)$$

which is a helix which rotates since, at fixed ϕ, $\theta = \omega t$ for m = 1 and constant displacement.

In toroidal geometry, technical reasons prohibit the insertion of helical windings into the torus. We have therefore constructed a series of horizontal antennae inside the vacuum vessel. With such an arrangement there will be simultaneous excitation of both m = +1 and m = -1 modes, rotating in opposite directions. The real displacement due to these two modes is

$$\xi_{real} = \xi_o \sin(n\phi + \omega t) \sin\theta$$

which is no longer a rotating motion but a simple oscillation.

Theory predicts that in toroidal geometry, modes with different values of m are coupled together, and we will therefore be exciting m = $\pm$2, m = $\pm$3, etc. Each mode has a corresponding resonant layer in which energy is dissipated, and this situation favours a more even distribution of absorbed power. The most favourable mode n-number is n = 2 and this is ob-

tained with four antenna groups situated 90^{o} apart around the torus in the toroidal direction. Each group consists of three slightly curved stainless steel plates connected to the exterior through ceramic insulators at the inside and outside of the top and bottom of the torus (Fig. 3). In addition a pair of vertical plates, at torus potential, shields each antenna group by cutting across the field lines.

The antenna system is powered by a generator of 2 MW which provides 1.0 MW into the plasma, given a 50% efficiency, which represents about four times the estimated ohmic dissipation in the plasma (plasma current 130 kA, loop-voltage $\sim$ 1.8V). Some important parameters are :

frequency = 3 MHz for $\bar{n}_e$	= 2.5 10^{13} cm^{-3} of deuterium
reactive power	= 12 MVA
peak current per antenna group	= 1.5 kA
peak voltage applied	= 2 kV
plasma oscillation ξ_o	< 0.5 mm

The programme to be followed will be to:

(1) Calculate the excitation level of different modes for a given antenna configuration. Look into the distribution of the dissipated power.
(2) Investigate any possible loss of plasma confinement caused by the heating. Pump out has been observed in various heating schemes e.g. ICRH at Kyoto {15} and Alfvén heating at Wisconsin {16,17}. In cylindrical geometry a theory developed at Kyoto {18} shows that the first order non linear interaction between the m = +1 and m = -1 mode drives a radial plasma flux. It is however, difficult to apply this theory to toroidal geometry. (3) Study the plasma behaviour near the resonant surfaces. The plasma will become turbulent and it is believed that destabilization will occur if the heating power is too high. We shall also study the frequency range where there is a danger of parametric excitation of certain modes.

3. Tokamak Parameters

According to the objectives stated in section 1., the machine was designed to satisfy the following conditions :

(1) The electron temperature must be sufficiently high ($T_e \gtrsim 500$ eV) to permit soft X-ray measurements.

(2) The duration of the discharge should be as long as possible such that a quasi-steady state can be established and the effect of r.f. heating can be observed.

(3) The machine should have a low aspect ratio ($R/a \sim 3$) in order to be able to reach high values of β and to test stability limits for plasmas with non-circular cross section (Phase II).

(4) The toroidal field coils must be demountable and elongated in the vertical direction such that the vacuum chamber can be easily replaced (Phase II).

It can be shown {19} that these conditions are compatible with a design based on the following essential parameters :

Major plasma radius	R	= 60.5 cm
Minor plasma radius	a	= 18 cm
Toroidal magnetic field on axis	B_T	= 1.5 Tesla

Using well-known scaling laws {20,21}, we can then derive typical expected plasma parameters :

Average electron density	$\bar{n}_e$	$\simeq 2.5\ 10^{13}\ cm^{-3}$
Peak electron temperature	$\hat{T}_e$	$\simeq$ 500 eV
Plasma current ($q_a \gtrsim 3$)	I_p	$\lesssim$ 135 kA
Electron energy confinement time	τ_{E_e}	$\simeq$ 2 ms

4. Toroidal Field Coil

The design of the TCA toroidal field coils is based on the same principles that were used for the design of the ISX coils at Oak Ridge {22}. These principles are :

(1) The coils are demountable such that the inner components of the machine (vacuum vessel, OH coils, vertical field coils) can be removed vertically.

(2) The coils are made from copper plates having sufficient structural strength to withstand all forces during operation {23}.

(3) The joints are located close to the points where the bending moment is zero {23}.

(4) The net centering force on each turn of the coil is taken up by a central fibreglass column.

(5) Out-of-plane forces, which arise from the interaction between the vertical field and the currents in the horizontal sections of the toroidal field coil {24}, are taken up by a stainless-steel machine frame.

(6) The coil is large enough to accommodate an elongated vacuum vessel (possible Phase II).

(7) The cooling system is designed in such a way that steady state operation at full field is possible at a rate of one shot every 5 minutes. A cooling power of 120 kW is installed.

Coil dimensions are shown in Fig. 4. The coils are constructed from 15mm thick copper plate. There are 72 turns, grouped in 18 bundles of 4 turns each. The maximum current is 66 kA, which produces a toroidal magnetic field of 15 kG at R = 60 cm. The stress calculations and heat transfer analysis are summarized in Ref. {23}. The maximum stress in the copper under normal operation is calculated as 60 N/mm^2.

The toroidal field coils and the associated machine support structure (shown in Fig. 5) have been constructed at the Eidgenössisches Institut für Reaktorforschung, Würenlingen, Switzerland. A team from the EIR also erected these components in Lausanne.

Power Supply : After considering various options, a power supply using a hexapolar diode rectifier connected to a 50 kV grid via two transformers has been selected. Switching is performed at 20 kV by means of mechanical circuit breakers. The current can be varied in steps by changing the voltage on the primary of the rectifier transformer. The available voltages are : 20, 15, 10, 5, 2 and 1 kV giving on axis toroidal fields of 15, 11.25, 7.5, 3.75, 1.5 and 0.75 kG respectively.

Typically the current pulse is initiated by closing the main switch at full voltage. The current rises to its maximum value in 2.0 secs. and remains constant for 0.2 secs (variation less than 2%). Thereafter, the switch is opened and the current decays exponentially with a time constant of 0.9 secs. In case of a switch failure there are various safety devices to protect the coil from over-heating.

5. Ohmic Heating System

Flux Swing Requirement

The inductive flux swing required to induce the plasma current I_p is given by $\phi_i = L_p I_p$, where L_p is the plasma inductance. Assuming a circular plasma with R = 60.5 cm, a = 18 cm, we have L_p = 1.2 μH and, taking I_p = 133 kA we obtain ϕ_L = 0.16 Vs. The resistive flux swing during the current build-up phase can be estimated from measurements on existing tokamaks. We estimate for TCA $\phi_{Bu} \tilde{=} 0.28$ Vs. Finally, the flux swing which is necessary to maintain the plasma current during the flat top phase (100 ms), assuming a loop-voltage of 1.8 Volts is ϕ_{FT} = 0.18 Vs. The total flux swing requirement is therefore ϕ = 0.46 Vs.

Ohmic Heating Coils

Due to the small aspect ratio and hence compact nature of the machine, the space required for an iron core is not available. The OH system will therefore operate with an air core and the stray fields produced in the plasma region by the primary OH coil must be compensated by the strategic placement of supplementary coils. This problem is accentuated by the fact that the OH transformer is initially at full current and the controlled current decay in the primary drives the plasma current. The effect of this is that the stray fields due to the coil are maximum when the plasma current is minimum.

The treatment of this problem is fully described in ref. {25}. The resulting coil configuration has since been modified due to technological problems with Coil C (see Fig. 3, ref. {25}). The final design of the OH system comprises a large cylindrical Coil (A in Fig. 6) and 4 auxiliary coils (B and D) which are all connected in series and powered by a single supply. The coils are wound from copper of rectangular cross section

insulated with fibre glass and potted in epoxy resin. The windings are hollow to allow water cooling of the coils.

The coils labeled E in Fig. 4 are powered separately (Fig. 7) and are used for final zeroing of the stray field in the plasma region. A stray field plot is given in (Fig. 6). These coils are pulsed on only for the critical breakdown phase when the feedback cannot properly control the plasma. These coils are also used to minimize reflected fields (from reinforced concrete floors) and for adjustment of the quadrupole fields.

Ohmic Heating Control Circuits

The circuit used to supply the current in the ohmic heating transformer coils is shown in Fig. 8. The main values in this circuit are :

C_1	-	40 mF	6 kV	720 kJ
C_2	-	140 µF	20 kV	28 kJ
L_e	∿	9.1mH		
R_e	∿	48 mΩ		

The functioning of the circuit is as follows (see Figs. 8,9) :

(i) Phase A. Ignitron I_1 is fired and the energy of the bank C_1 is transferred to the OH coil inductance during the quarter-cycle time of 30.0 msecs. During this phase there is an effective loss of flux due to the internal resistance of the transformer coil, which amounts to 8%. The final stored current can be up to 11.5 kA.

(ii) Phase B. At the end of phase A, the bank C_2 is fired into the circuit by ignitron I_2 and causes the current in S_2 to cross zero, at which time the arc in S, is extinguished, S_1 being a vacuum switch, V5 of GEC Ltd. At the same time ignitron I_3 is automatically fired. After this time, the stored current can only pass through

R_2+R_1 giving a fast decay and hence a large value of induced e.m.f. around the torus (~100V). This causes the partially preionized gas in the torus to build up into a plasma current, further ionizing the background gas.

(iii) Phase C. As soon as the current build-up starts, the ignitron I_4 is fired, shorting out R_1 and reducing the decay rate of the primary current, and hence reducing the volts/turn on the plasma and the rate of current rise.

(iv) Phase D. When the current nears its required value, ignitron I_5 is fired (S_3 shut) bringing R_3, R_4 and R_2 all into parallel. This results in a still smaller volts/turn and produces a slowly changing maximum in the plasma current.

(v) Phase E. After a certain time (dependent on the plasma resistive voltage) the current has fallen below its peak. I_7 is now fired to cancel the current in S_3 which is opened, increasing the decay resistance. The increased volts/turn produces a second current peak, of similar value, but of shorter duration.

(vi) Phase F. Still later the switch S_2 is opened firing I_6, leaving only R_3 in the circuit. The volts/turn again increase giving a third and still shorter peak. The current then drops faster and faster while the plasma cools and finally decays due to the lack of the ohmic heating power.

The resistors R_2, R_3 and R_4 are continuously variable liquid resistors. By varying these, and the exact timing of the whole sequence, we can produce a variety of current waveforms.

In addition, we intend in 1980 to add a feedback component to the Ohmic Heating circuit, to suppress the ripple due to the switching of the circuit.

6. Vertical Field Coil System

The vertical and horizontal fields necessary for the equilibrium and positioning of the plasma are produced by a system of 8 coils placed around the plasma (F, G and H, Fig. 6). The positions of these coils were calculated such that the curvature index of the vertical magnetic field ($n = \frac{-R}{B_v} \partial Bv/\partial R$) in the plasma region has a value $0 < n < 3/2$ thus ensuring basic stability of the plasma column. The map of the field index is shown in Fig. 10. A further constraint on the positioning of these coils was that they should not obstruct access to the vertical and radial viewing ports on the torus. The coils are connected in series with the sense of the currents in F,G and H opposed, such that the voltage induced into the system by coupling to the OH circuit is minimized.

The vertical field coils have been constructed in the same manner as the OH coils, but do not need water cooling due to the low power requirements.

7. Transverse Field Power Supplies

The eight coils providing transverse fields in the plasma region are interconnected in such a way as to produce four different field configurations : vertical field, horizontal field, quadrupole field and an oscillating transformer flux for discharge-cleaning and preionization. Fig. 11 shows the complete system.

The sum of the currents from amplifiers A_1 and A_2 determines the vertical field on axis and their difference determines the horizontal field. These amplifiers are fed by two electrolytic capacitor banks in series, each one a 400V bank. The main bank of 4 Farad (320 kJ) produces the currents for the flat-top phase of the plasma current, for which 400 Volts is sufficient. The additional smaller (40 mF) bank discharges quickly but provides an additional 400 Volts during the plasma current rise, when a greater inductive voltage is required to build up the current in the control windings. This small bank is bridged by a diode when it has discharged. Initially a current rise of 800 A/msec can be induced in the control windings, corresponding roughly to a plasma current build-up of $\sim$ 50 kA/msec. The peak current delivered by the amplifier is limited to 2000 A, giving $\sim$ 700 Gauss vertical field on axis, corresponding to $\sim$ 130 kA plasma current. The individual coils are composed of ten turns each. It should be remembered that the vertical field on axis inside the vacuum vessel will rise at a slower rate than the simple calculation, due to the shell time constant of $\sim$ 1 msec.

At full toroidal field, the current maximum limits the maximum β_θ controllable. In fact β_θ is limited to q_a-2 approximately. Thus at q=4 a poloidal β of 2 could still be in equilibrium.

The double amplifier has been developed and constructed in collaboration with the Schweizerischen Institut für Nuklearforschung (SIN). It is based on the principle of a variable resistor comprising many resistors in parallel, switched by transistors. Each amplifier consists of 140 groups of transistors plus resistors which are switched in a given order providing an almost continuously variable resistance. The resistances are dimensioned such that the resistance changes on a logarithmic scale. The number of transistors switched is determined by an ADC referencing an analogue control input. An internal feedback loop then assures that the output voltage is indeed proportional to the input signal (Gain = 200), and the complete amplifier thus behaves as a high-power voltage amplifier at zero impedance. This feature allows us to use the transverse field

coils independently for vertical, horizontal and quadrupole fields.

It is important to note that the amplifier is permanently on and provides the full control field during current rise, flat-top and current descent. The current descent can only be followed for a limited slope of up to 15 kA/msec, a quarter of the maximum rate of rise.

The quadrupole field current I_q is produced by a damped capacitor discharge (Fig. 12). This circuit provides a peak of up to 1200 A and a pulse-width of $\sim$ 6 msec, corresponding to a quadrupole field of roughly $\pm$ 50 Gauss at the limiter radii and 1.6 Gauss/cm on axis. This field is applied just prior to the application of the loop-volts to break down the plasma, such that it reaches a maximum at the instant of breakdown. The location of the quadrupole null is variable by means of the trimming OH coils E_T and E_B (Section 5).

8. Vacuum System

The toroidal vacuum chamber (Fig. 13) is built from 316 LN stainless steel, by Aluminium Schweisswerk AG, Schlieren. The interior is roughly square in cross-section (420 x 520 mm^2) and was polished mechanically after which it was chemically cleaned. The side walls are 5 mm thick and the top and bottom walls are 12 mm thick. The torus is made in two halves, isolated electrically to permit the penetration of the field produced by the ohmic heating transformer. The vacuum seals are made from two square Viton rings with differential pumping. The large flanges joining the two halves are water-cooled.

The torus is well equipped with ports. There are 4 radial ports for pumping and 18 for diagnostic measurements. In the top and bottom of the vessel there are 10 long ports to view the complete plasma diameter, plus 12 extra ports. In addition there are 80 ports for the insertion of various Alfvén heating antenna configurations. All ports are constructed using standard conflat flanges.

The pumping system consists of two sets of turbomolecular pump + titanium getter pump plus two extra titanium getter pumps. The total pumping speed at the torus should be in excess of 1000 1/sec. This should give us a base pressure better than 5×10^{-9} torr, taking outgasing of the Viton and the stainless steel into consideration. The whole torus can be shut off completely by valves using gold seals. The limiters are made from stainless steel to begin with, and can be moved individually, thereby changing plasma diameter and position.

High- and low-pressure mass-spectrometers are built into the system. Gas inlet is by four Veeco PV-10 piezo-electric valves. These will eventually be controlled by feedback from the central chord density measurement. Four movable limiters are positioned in one sector forming a rectangular aperture. These limiters are constructed from 304 L stainless steel.

9. Discharge Cleaning and Preionization

Discharge cleaning in a Tokamak has two functions, firstly to heat the walls, thereby liberating gases, especially water vapour, buried in the wall, for which as high a temperature as possible is required, and secondly, to chemically remove impurities, mainly oxygen and carbon, by the interaction of highly reactive atomic hydrogen with the wall,

for which as low a wall temperature as possible is required. An electron temperature of 2 - 3 eV has been recognized as suitable in previous experiment {26}. The discharge is created by an induced loop-voltage produced by a 100 kW pulsed oscillator, operating at 5 kHz. The pulse duration can be varied from 5 to 20 msec , and the repetition rate from 1 to 5 Hz. In this way a pulsed plasma current of 1.5 kA is produced, and the average dissipated power can be controlled in order to avoid wall overheating. A constant but variable small toroidal magnetic field of up to 500 Gauss is applied during discharge cleaning. The cleaning loop-voltage is induced by an external coil. The same coil produces during the experiment the vertical stabilizing field and the quadrupolar initial field. Pneumatic switches commutate the circuits. By a suitable switching, the same oscillator which produces the cleaning current before the experiment is used, at the beginning of the experiment, to produce an initial preionization of the filling gas before the OH pulse is applied. This reduces the volt-seconds of transformer flux to build up current flat-top to the current peak. The frequency of the preionization pulse is 16 kHz, the breakdown will be obtained after a few cycles. Electric filters are used to separate the preionization and the vertical field circuits. The circuitry of the cleaning-preionization device is shown in Fig. 4.

10. Diagnostics

TCA will be equipped with a set of diagnostics which will enable the measurement of the various parameters of the discharge. The following measurements are being prepared and their location on the torus is shown in Fig. 15.

I) Electromagnetic diagnostics: The plasma loop-voltage will be measured by a simple toroidal pickup-loop located outside the vacuum vessel. The plasma current will be measured by Rogowski coils and the position of the centre of the plasma current distribution will be monitored by a set of modified sine-cosine coils. These coils have been modified in such a way that toroidal effects have been minimized and the output is linear with respect to the displacement from an arbitrary centre position. Average values of B_R, B_V and B_ϕ will be measured by a set of orthogonal pick-up coils. Sin 2θ and Sin 3θ coils have also been included to give information on the plasma shape. The plasma beta will be measured using a diamagnetic loop. All of the above diagnostics, except the voltage-loop, are housed in a pair of cradles which encircle the plasma outside the vacuum vessel.

II) Electron Density: Line-integrated electron density is measured along a single vertical chord, close to a diameter, by means of a 140 GHz microwave interferometer. This system uses a low power (8.5 mW) Gunn-oscillator source and is designed to produce a linear total phase-shift analogue output for use with the gas-feeding. Overmoded waveguide (X-band) is used between interferometer and Tokamak, and also serves as the antennae, across quartz vacuum windows.

The electron-density profile is measured by an eight-channel optical interferometer. This uses an optically-pumped Methyl Iodide laser at 447 μm. This diagnostic is being prepared by the CRPP Laser Group, using a previously studied technique {27}.

III) Ruby-Scattering: The electron-temperature profile is measured at one point at a time along a horizontal diameter by conventional Thomson scattering of ruby-laser light. The laser system provides two separate pulses (later four) and the detection system is based on a multi-channel fibre-optic image dissector. This diagnostic is being prepared by the CRPP Laser Group, along the lines of a previous proven system {28}.

IV) Spectroscopy : The absolute emission of the H_α light (6563 Å) is measured at various positions and tells us the volume ionization rate from which the electron confinement time is inferred. A fast radial scanner is also under construction. A set of spectroscopic measurements on the low ionization levels of Iron, Carbon and Oxygen (the main impurities) will enable the qualitative behaviour of these atoms to be studied. This is performed using narrow band interference filters of wavelengths of 4415, 2600, 4646, 3920 Å.

V) Ion-temperature: The ion temperature is measured via the neutral atom emission spectrum, using a five-channel NPA purchased from the USSR {29}. This can be scanned in a vertical direction for radial profile measurement, and also in a horizontal direction. As well as this a simple, one channel high-energy analyzer is being constructed with the specific aim of looking at the tail of the energy spectrum during the heating pulse. This single energy device can observe the plasma almost tangentially. In addition, the laboratory is preparing to measure T_i by means of Far Infra Red collective scattering. This experiment is being carried out by the CRPP Laser Group.

VI) Soft X-ray diagnostics:

(a) An array of 7 pairs of surface barrier diodes (ORTEC CA-15-100-300) will be mounted in vacuum to view the plasma in a horizontal direction through a 25 μ B_e window. This measurement will give the electron temperature using the ratio method, for seven different chords. Thus we have a time resolved measurement of the temperature profile. To improve the accuracy of the ratio method the array can be increased to 7 x 3 diodes giving 3 measurements of T_e per chord. It is also possible to move one set of diodes with respect to the other allowing the possibility of viewing 14 chords simultaneously for mode and fluctuation measurements.

(b) Two fixed diode pairs will view the plasma in a vertical direction to give a permanent monitor of T_e, however with lower spatial resolution than the 2 x 7 array.

(c) An array of 3 diodes will be mounted on the same slit port as (b). This array will view 3 chords in the central region of the plasma. The resolution will be high and it will be used to monitor the position of the magnetic axis, it could eventually be used for position feedback as well as providing a good measurement of the axis for Abel inversion calculation (e.g. for the FIR interferometer).

(d) A high resolution diode will be placed in a different toroidal sector directly under the Alfvén wave antennae. As well as giving toroidal mode information it may be possible to monitor plasma edge motion due to the Alfvén waves.

(e) A Si(Li) X-ray spectrometer is foreseen to monitor the X-ray spectrum up to $\sim$ 20 keV. This will be an average over many shots as the MCA will not be fast enough for fast sampling. As well as giving an average T_e it will be used to monitor the impurity lines present that could affect the ratio measurements (a,b) and also to monitor fast electrons that may be generated when heating the plasma.

(f) In collaboration with the University of Lausanne the possibility of installing a multiwire proportional counter is being studied. Using an MWPC it may be feasible to perform many channel imaging of the spatial emission distribution across the plasma cross section.

VII) Hard X-rays: A simple hard X-ray monitor will be set up to observe the forward angle X-rays from the limiter, this will serve as an indication of the nature of the discharge. From a health physics point of view pen dosimeters and film badges will monitor the hard X-radiation at various strategic positions in the laboratory.

VIII) Electron Cyclotron Emission: A Fourier transform interferometer (of the type used by Costley et al). {30,31} will be installed to monitor the ECE from the plasma. Using this instrument it will be possible to obtain a complete ECE spectrum and thus a $T_e(r)$ profile every 15 - 20 msec. A dual channel QMC detector has been foreseen and the possibility of using the second channel to monitor a fixed frequency continuously in time using a Fabry Perot frequency selector is being studied.

11. Machine Control

The control of the Tokamak and its power supplies is performed completely by software with the exception of one global hard-wire safety interlock. A distributed processing network has been developed in the laboratory to carry out this function and the total system is shown in Fig. 16. Each subsystem is controlled by its own microprocessor under local or remote command. A central unit communicates with all remote units and performs the control functions. In addition a separate unit controls the display of all information for the operators via a TV screen. The Motorola 6800 microprocessor is used throughout and individual units communicate via commercial fibre-optic links using the EIA RS232 protocol. A slightly modified version of the EPFL "MUBUS" is used as a backplane for the circuit cards in all units. All cards were developed in the laboratory and include: a processor card, memory cards (2K, 8K of RAM and 8K of ROM) standard I/O card (ACIA), special interface card (PIA and ACIA) and timer card.

The experiment cycle sequence timer has been specially developed using a three-channel timer circuit giving timing intervals from 3 μsec to 2.5 hours. The timing intervals are by thumbwheel switches and their values are remotely readable.

12. Data Acquisition

The majority of information from diagnostic equipment appears in the form of analogue signals. These are digitised by a DATEL DAS250 ADC unit which sample at 4 μsec intervals while multiplexing up to 16 channels, giving 250 kHz sampling rate for one channel and up to 15 kHz for 16 channels. Normally a sampling rate of 2 kHz is foreseen. The digitised information is stored via a DMA channel onto local memory. Such units can operate alone, with an analogue output "refresh" capability or they can be read out by the standard EIA terminal interface.

A layout of the acquisition and display system is included in Fig. 16. The central computer is a PDP 11/60 which communicates with all the acquisition units independently, as well as with the timer units. VDU screens are available for evaluation of experimental data and a plotter produces graphical hard-copy output. A graphics package {32} has been written to facilitate the use of the output devices. The data transfer programme {33} has been specially written to coordinate the retrieval of data from all the remote microprocessor-controlled acquisition units. It is expected that this transfer should take less than 10 seconds, and it is limited by the speed at which data can be dumped on to disk.

This programme is greatly simplified by being written entirely in FORTRAN and also by only allowing one standard remote module communication protocol. All the standard compatibility problems are thereby displaced into the software of the remote units.

../22

13. State of Construction (Dec. 79)

The decision to build the TCA Tokamak was taken in September 1977. Since that time, the project has evolved through its various phases (design, acquisition, construction) and considerable progress has been made. As of December 1979, all major components have been delivered to the site and assembly of the machine is approximately 50% complete (Fig. 1).

The toroidal field coils have been assembled and will be tested shortly. The OH and vertical field coils have been installed and the OH power supply is presently under construction at CRPP. The vertical-field power supply will be ready in February 1980. The torus has passed its first vacuum test recently and the Alfvén antennae have been installed. Diagnostic devices are in various stages of construction; basic diagnostics should be ready by March 1980. The PDP 11/60 computer to be used for data acquisition has been in operation for some time.

Starting in January 1980, the various systems of TCA will be tested and Tokamak operation should be possible in the first half of 1980.

14. Acknowledgements

This work is supported by the "Fonds National Suisse de la Recherche Scientifique", by the "Nationaler Energie Forschungs-Fonds", by the "Ecole Polytechnique Fédérale de Lausanne" and by Euratom.

15. References

{1} Blanc, P., Hess, W., Ichtchenko, G., Javel, P., Lallia, P., Mahn, C., Nguyen, T.K., Ohlendorf, W., Pacher, G.W., Pacher, H.D., Takamura, S., Tonon, G., Wegrowe, J.G., Plasma Physics and Controlled Nuclear Fusion Research (Proc. 6th Int. conf. Berchtesgaden, 1976) Vol. III, IAEA Vienna 1977, 49.

{2} Equipe TFR, loc. cit., 39.

{3} Buzankin, V.V., Vershkov, V.A., Ivanov, N.V., Kovan, I.A., Krupin, V.A., Popov, I.A., Semenov, I.B., Sokolov, Yu. A., loc. cit., 61.

{4} Bol, K., Cecchi, J.L., Daughney, C.C., DeMarco, F., Ellis, R.A., Eubank, H.P., Furth, H.P., Hsuan, H., Mazzucato, E., Smith, R.R., Plasma Physics and Controlled Nuclear Fusion Research, (Proc. 5th Int. Conf. Tokyo, 1974) Vol. I, IAEA, Vienna 1975, 83.

{5} Berry, L.A., Bush, C.E., Dunlap, J.L., Edmonds, P.H., Jernigan, T.C., Lyon, J.F., Murakami, M., Wing, W.R., loc, cit., 113.

{6} Equipe TFR, Plasma Physics and Controlled Nuclear Fusion Research (Proc. 6th Int. Conf. Berchtesgaden, 1976) Vol I, IAEA Vienna 1977, 69.

{7} Eubank, H. Goldston, R., Arumsalam, V., Bitter, M., Bol, K., Boyd, D., Bretz, N., Bussac, J.-P., Cohen, S., Colestock, P., Davis, S., Dimock, D., Dylla, H., Efthimion, P., Grisham, L., Hawryluk, R., Hill, K., Hinnov, E., Hosea, J. Hsuan, H., Johnson, D., Martin, G., Medley, S., Meservey, E., Sauthoff, N., Schilling, G., Schivell, J., Schmidt, G., Stauffer, F., Stewart, L., Stodiek, W., Stooksberry, R., Strachen, J., Suckewer, S., Tait, G., Ulrickson, M., von Goeler, S., Yamada, M., Plasma Physics and Controlled Nuclear Fusion Research (Proc. 7th Int. Conf. Innsbruck 1978) Vol I, IAEA Vienna 1979, 167.

../25

{8} Swain, D.W., Bates, S.C., Bush, C.E., Colchin, R.J., Cooper, W.A., Dunlap, J.L., Dyer, G.R., Edmonds, P.H., England, A.C., Foster, C.A., Hogan, J.T., Howe, H.C., Isler, R.C. Jernigan, T.C., Ketterer, H.E., Kim, J., King, P.W., Lazarus, E.A., Loring, C.M., Lyon, J.F., McCurdy, H.C., Menon, M.M., Mihalczo, J.T., Milora, S.L., Murakami, M., Navarro , A.P., Neidigh, R.V., Neilson, G.H., Overbey, D.R., Paré, V.K., Peng, Y-K.M., Ponte, N.S., Saltmarsh, M.J., Schechter, D.E., Simpkins, J.E., Stirling, W.L., Thomas, C.E., Tsai, C.C., Wilgen, J.B., Wing, W.R., Worsham, R.E. and Zurro, B. . Controlled Fusion and Plasma Physics (Proc. 9th European Conf. Oxford, 1979) Vol I. EPS, Oxford 1979, 44.

{9} Pochelon, A. and Keller, R., Helv. Phys. Acta, 50 (1977), 172.

{10} Keller, R., CRPP Laboratory Report LRP 104/76, Lausanne 1976.

{11} Tataronis, J.A., J. Plasma Phys., 13 (1975), 87.

{12} Keller, R., Gruber, R. and Troyon, F., Heating in Toroidal Plasmas (Proc. Joint Varenna-Grenoble Int. Symp. 1978) Vol II. CENG Grenoble 1978, 195.

{13} Keller, R., Pochelon, A., Nuclear Fusion 18 (1978) 1051.

{14} Pochelon, A., CRPP Laboratory Report LRP 136/77, Lausanne 1977 (Thesis).

{15} Yasaka, Y., Itatani, R., Heating in Toroidal Plasmas (Proc. Joint Varenna-Grenoble Int. Symp. 1978) Vol I. CEN Grenoble 1978, 139.

../26

{16} Shohet, J.L., Talmadge, J.N., Tataronis, J.A., Grossmann, W., Hasegawa, A., Chen, L., Holzhauer, E., Janzen, G., Moser, F., Müller, G., Räuchle, E., Schneider, E., Schüller, P.G., Plasma Physics and Controlled Nuclear Fusion Research (Proc. 7th Int. Conf. Innsbruck 1978) Vol II, IAEA Vienna, 569.

{17} Golovats, S.N., Shohet, J.L., Phys. Fluids, 21 (1978) 1421.

{18} Yasaka, Y., Itatani, R., Nagoya University Research Report IPPJ-416, Nagoya 1979.

{19} Hofmann, F., Keller, R., CRPP Internal Report INT 86/77, Lausanne 1977.

{20} Murakami, M., Callen, J.D., Berry, L.A., Nuclear Fusion 16 (1976), 347.

{21} Hugill, J., Sheffield, J., Nuclear Fusion 18 (1978), 15.

{22} Hussung, R.O., Cousteau, D.C., Johnson, N., Engineering Problems of Fusion Research (Proc. 6th Symp. San Diego 1975).

{23} Hofmann, F., CRPP Internal Report INT 86/77, Lausanne 1977.

{24} Cheetham, A.D., Hofmann, F., CRPP Internal Report INT 82/77, Lausanne 1977.

{25} Cheetham, A.D, Hofmann, F., CRPP Internal Report INT 90/78, Lausanne 1978.

{26} Oren, L., Taylor, R.J., Nuclear Fusion 17 (1977) 1143.

{27} Veron, D., TFR Report EUR-CEA-FC-980, Fontenay aux Roses 1978.

{28} Prentice, R., Culham Laboratory Report CLM-R-179, Culham 1978.

../27

{29} Afrosimov, V.V., Berezovskii, E.L., Gladkovskii, I.P., Kislyakov, A.I., Petrov, M.P., and Sadovnikov, V.A., Sov. Phys. Tech. Phys., 20 (1975), 33.

{30} Costley, A.E., Hastie, R.J., Paul, J.W.M., Chamberlain, J., Phys. Rev. Lett. 33 (1974), 758.

{31} Costley, A.E., TFR Group, Phys. Rev. Lett. 38 (1977), 1477.

{32} Lister, J.B., Schreiber, R.S., CRPP Internal Report INT 96/79, Lausanne 1979.

{33} Schreiber, R.S., Lister, J.B., CRPP Internal Report INT 93/79, Lausanne 1979.

../28

16. Figure Captions

Figure 1 TCA Tokamak during assembly.

Figure 2 Cut-away diagram of TCA.

Figure 3 The Alfvén wave antennae structure.

a) section through the torus

b) from above

Figure 4 Diagram showing the structure and dimensions of a toroidal field coil packet.

Figure 5 The toroidal field coil support structure from above.

Figure 6 Section of TCA showing the positions of the poloidal field coils and the stray fields due to the OH coil at the beginning of the plasma pulse (contours are marked in gauss).

Figure 7 E Coil power supply circuit.

Figure 8 Ohmic heating circuit.

../29

Figure 9 Schematic waveforms for the OH Coil current (I_{OH}), the plasma loop voltage (V_L) and the plasma current (I_P).

Figure 10 Map of the vertical field curvative index ($n = -R/_{Bv}\ \partial Bv/_{\partial R}$) over the plasma region.

Figure 11 Transverse field power supplies.

Figure 12 Quadrupole field power supply circuit.

Figure 13 The vacuum vessel viewed from above and from the side.

Figure 14 Preionisation and discharge cleaning oscillator (5 - 16 kHz, 100 kW pulsed).

Figure 15 Schematic of TCA from above showing the layout of the diagnostics.

Figure 16 The control system.

TCA TOKAMAK DURING ASSEMBLY

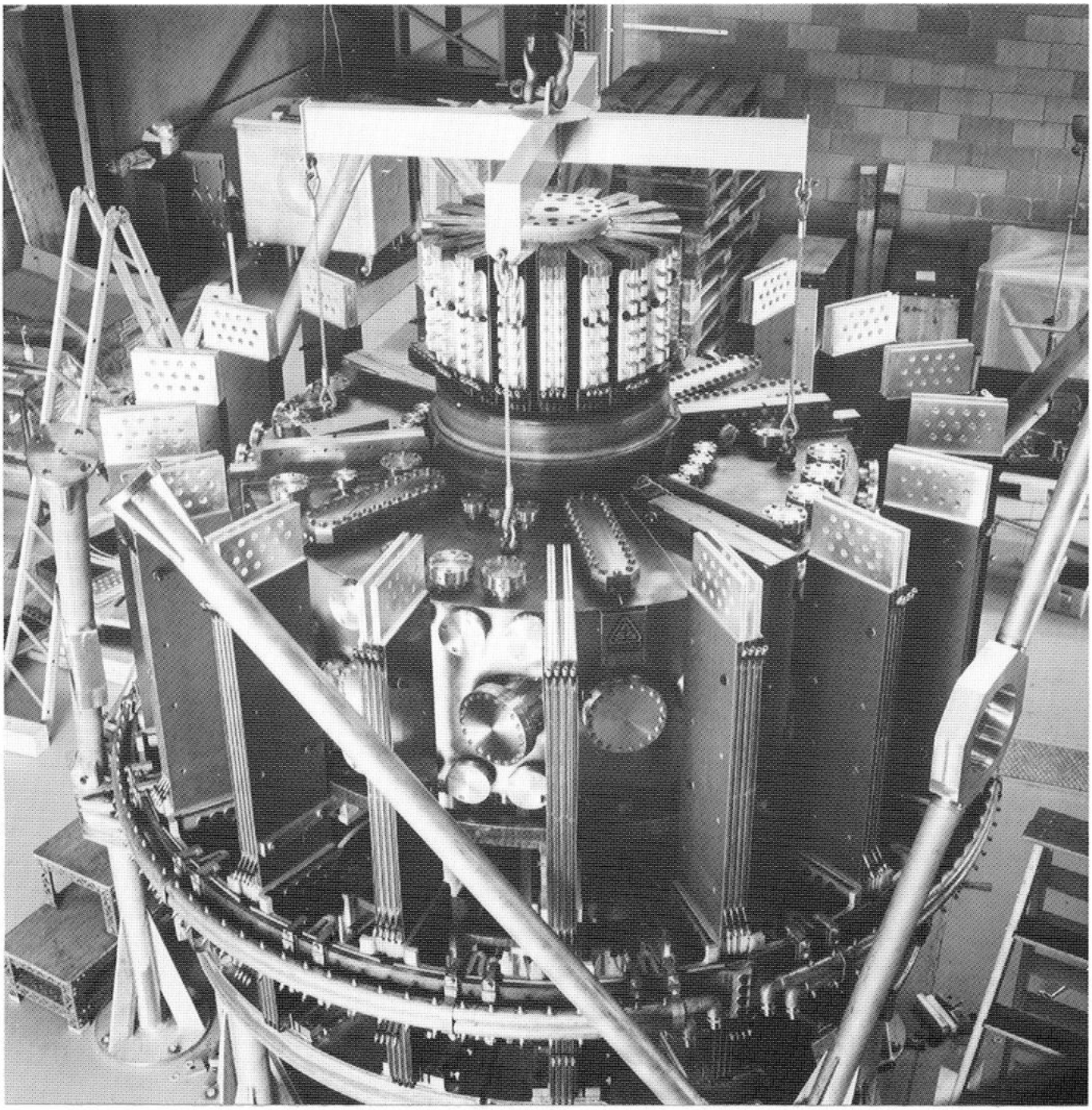

FIG. 1

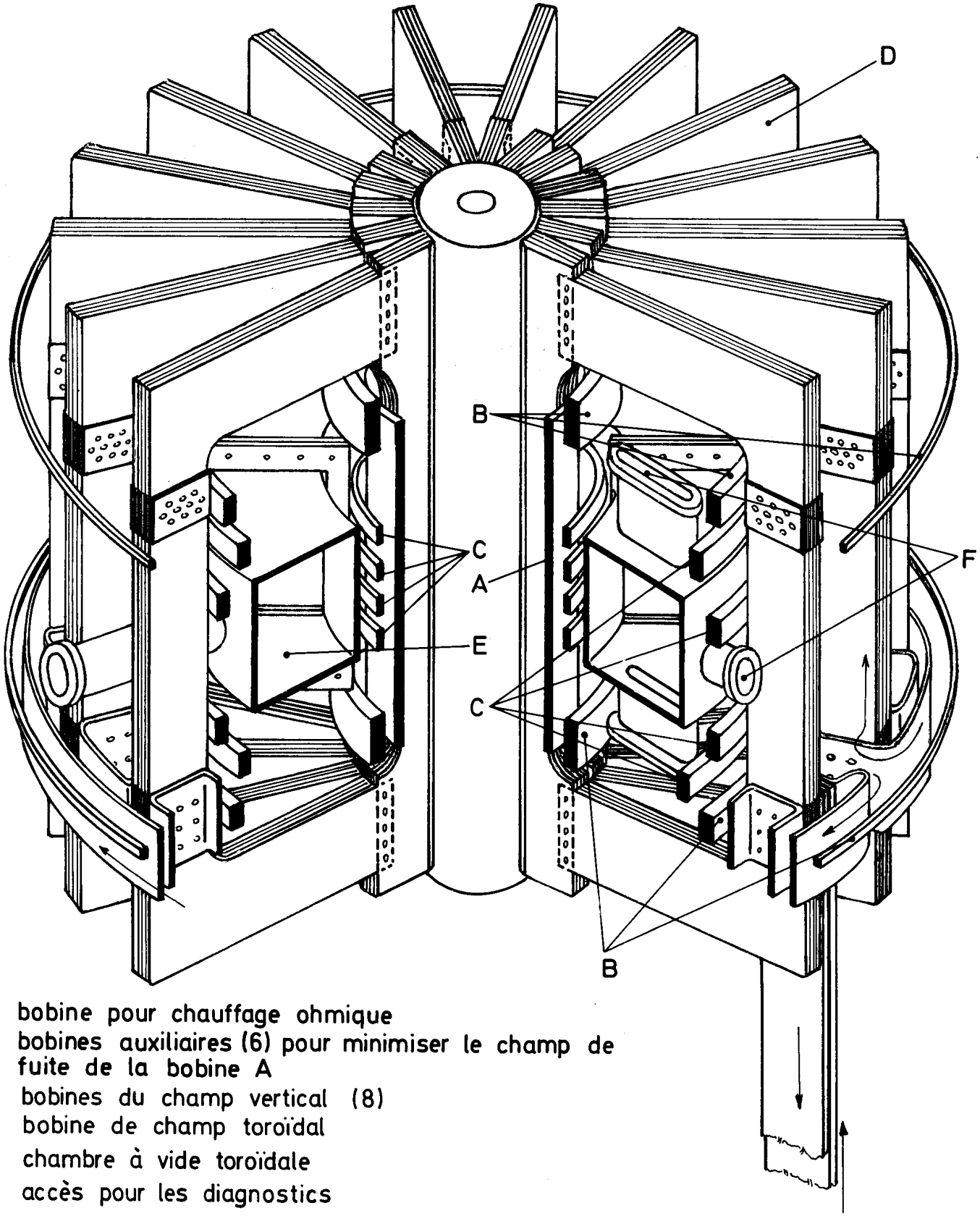

A bobine pour chauffage ohmique
B bobines auxiliaires (6) pour minimiser le champ de fuite de la bobine A
C bobines du champ vertical (8)
D bobine de champ toroïdal
E chambre à vide toroïdale
F accès pour les diagnostics

Fig. 2

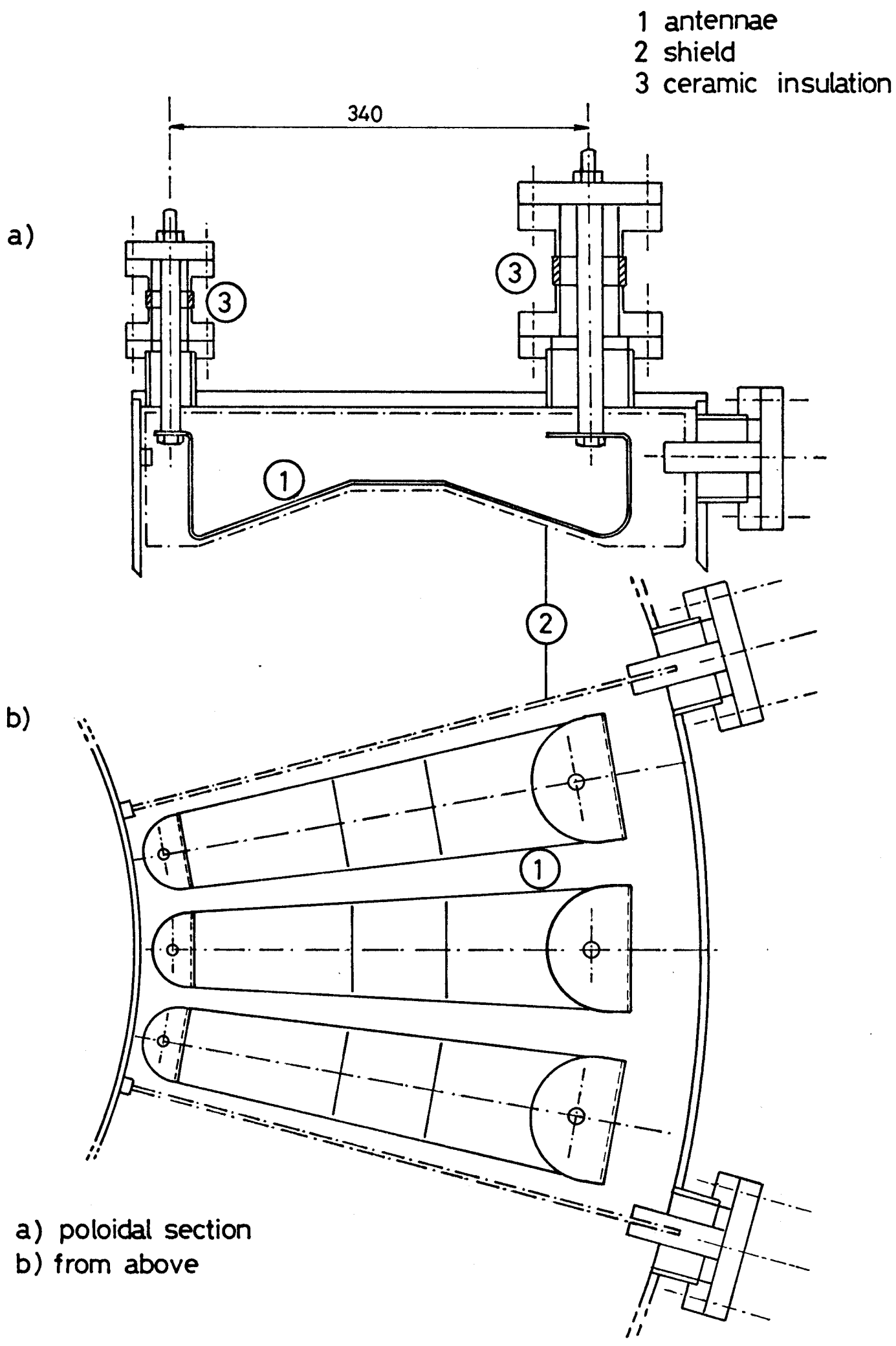

Fig 3 Alfvén Wave Antennae

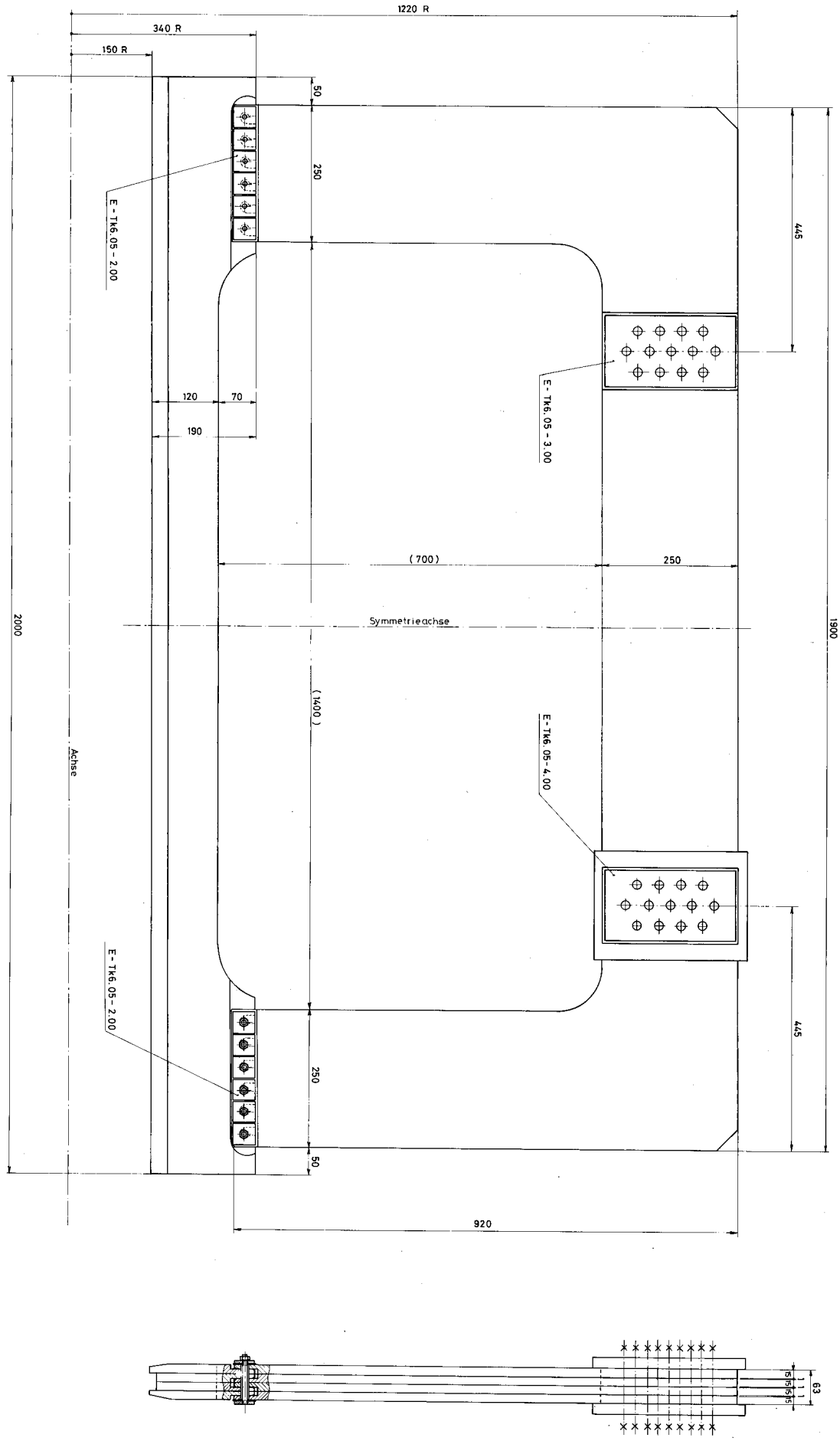
1220 R
340 R
150 R
50
250
E - TK6.05 - 2.00
445
120
70
190
E - TK6.05 - 3.00
(700)
250
Symmetrieachse
2000
1900
(1400)
E - TK6.05 - 4.00
Achse
E - TK6.05 - 2.00
250
445
50
920
15
15
15
15
63

Fig. 4

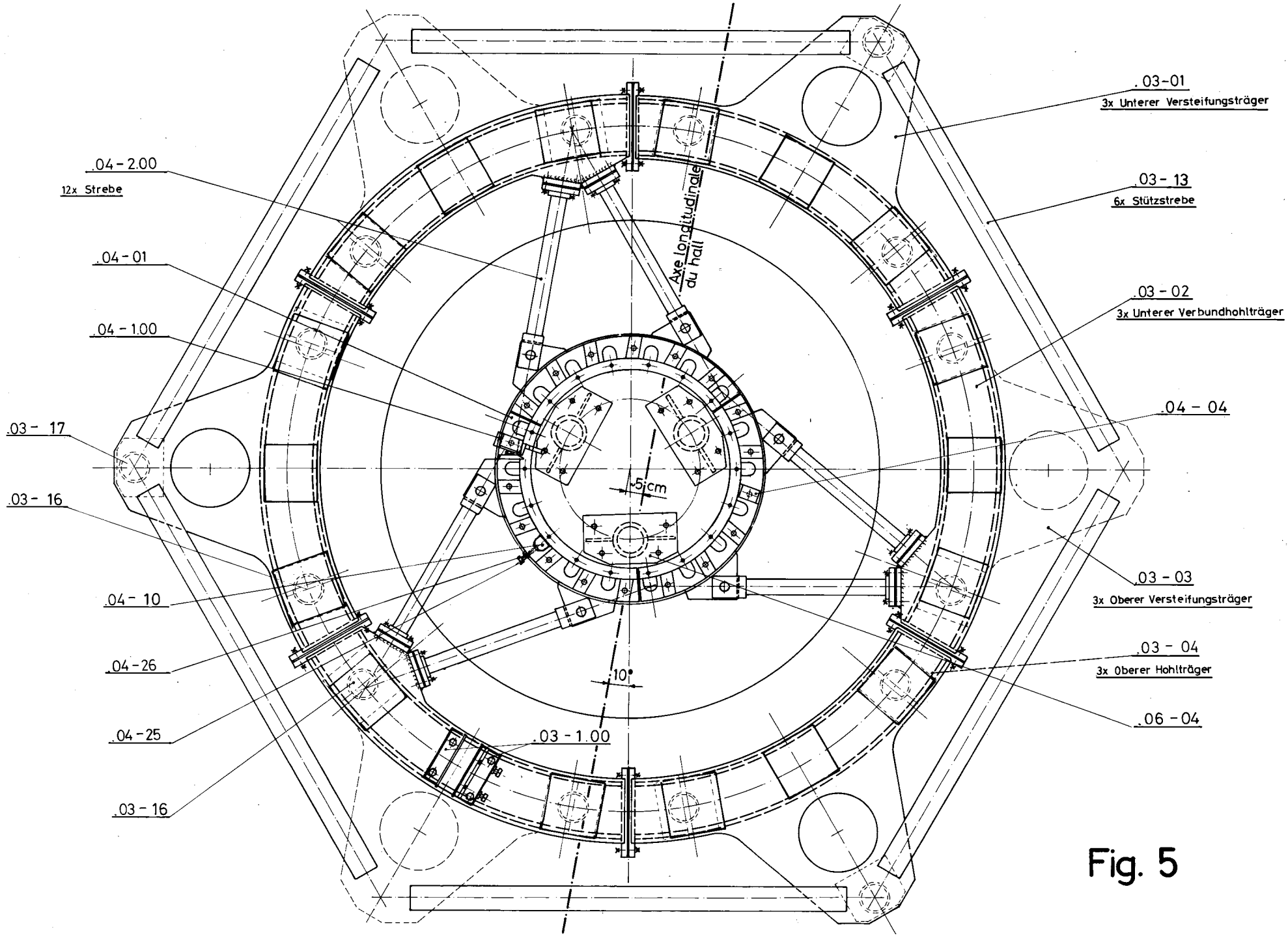
.03-01
3x Unterer Versteifungsträger
.03-13
6x Stützstrebe
.03-02
3x Unterer Verbundhohlträger
.04-04
.03-03
3x Oberer Versteifungsträger
.03-04
3x Oberer Hohlträger
.06-04
.03-1.00
.04-2.00
12x Strebe
.04-01
.04-1.00
.03-17
.03-16
.04-10
.04-26
.04-25
.03-16
Axe longitudinale du hall
5 cm
10°

Fig. 5

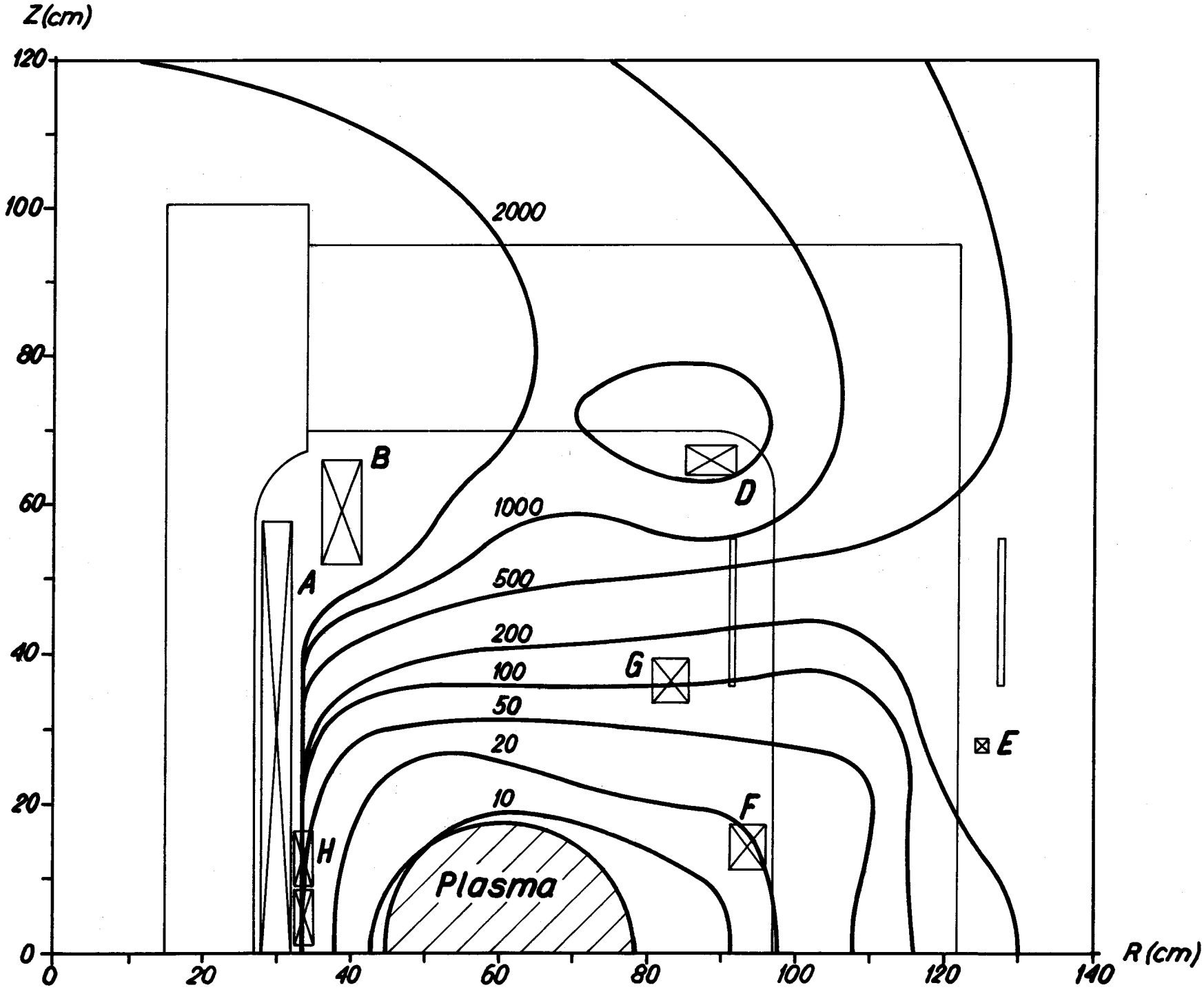
Z(cm)
120
100
80
60
40
20
0
0
20
40
60
80
100
120
140
R(cm)
2000
1000
500
200
100
50
20
10
A
B
D
E
F
G
H
Plasma

Fig 6

E COIL POWER SUPPLY

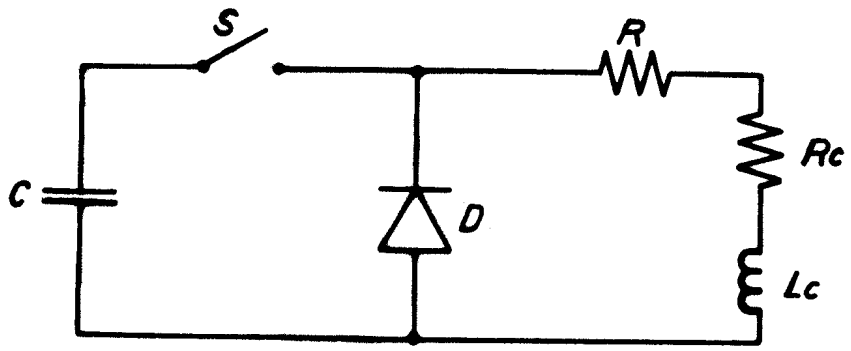

Fig 7

C	=	720	μF	(6kV)		
L_c	=	4	mH	Rise Time	=	2.3 msecs.
R_c	=	0.35	Ω	Decay Time	=	3.4 Msecs.
R	=	0.82	Ω			

D = Diode clamp (10kV 3kA).

S = EE BK7703 Ignition

Peak Current I_o = 1 kA for Charging Voltage of V_o = 3.44 kV

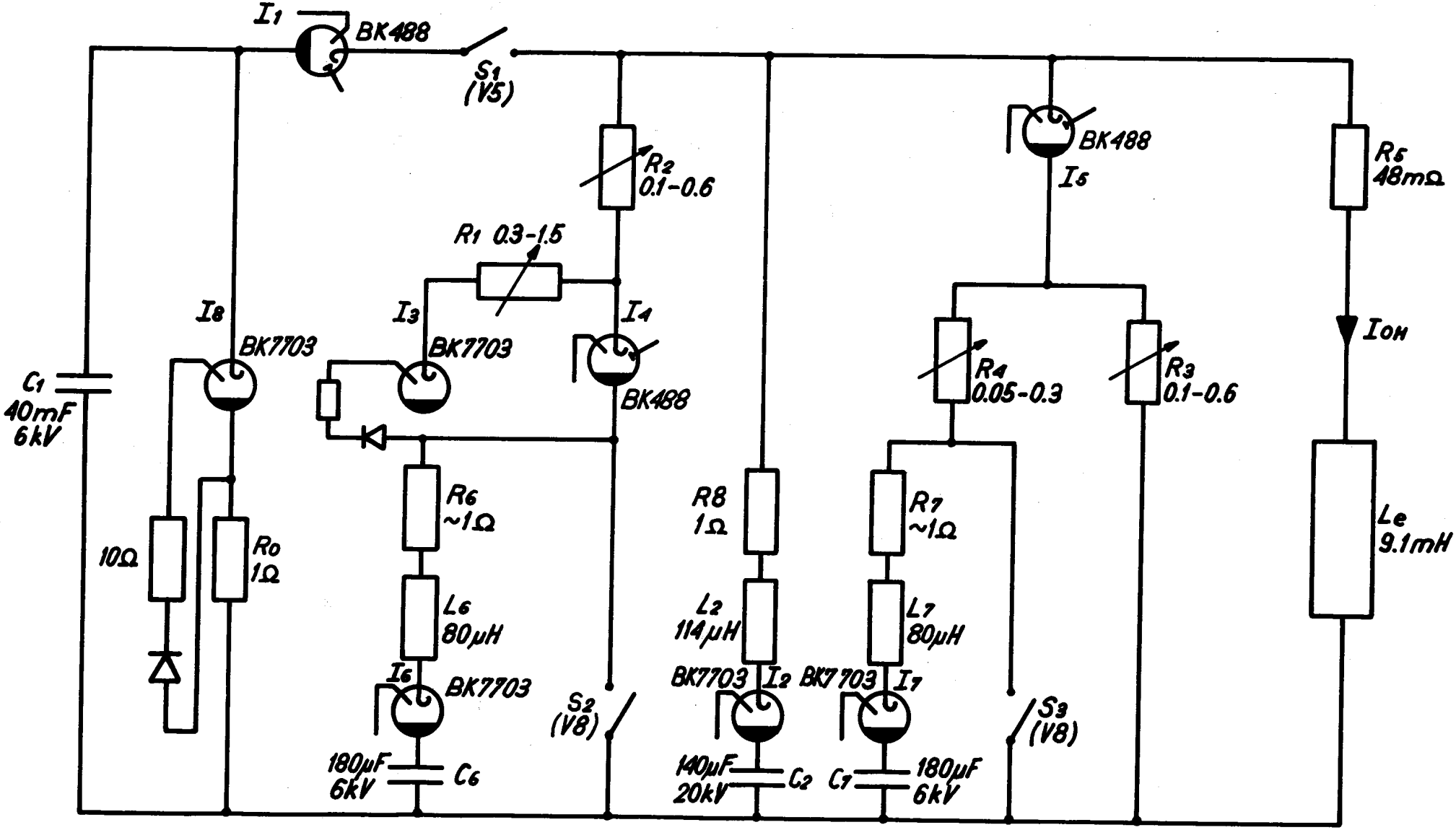

Fig.8 Ohmic heating circuit

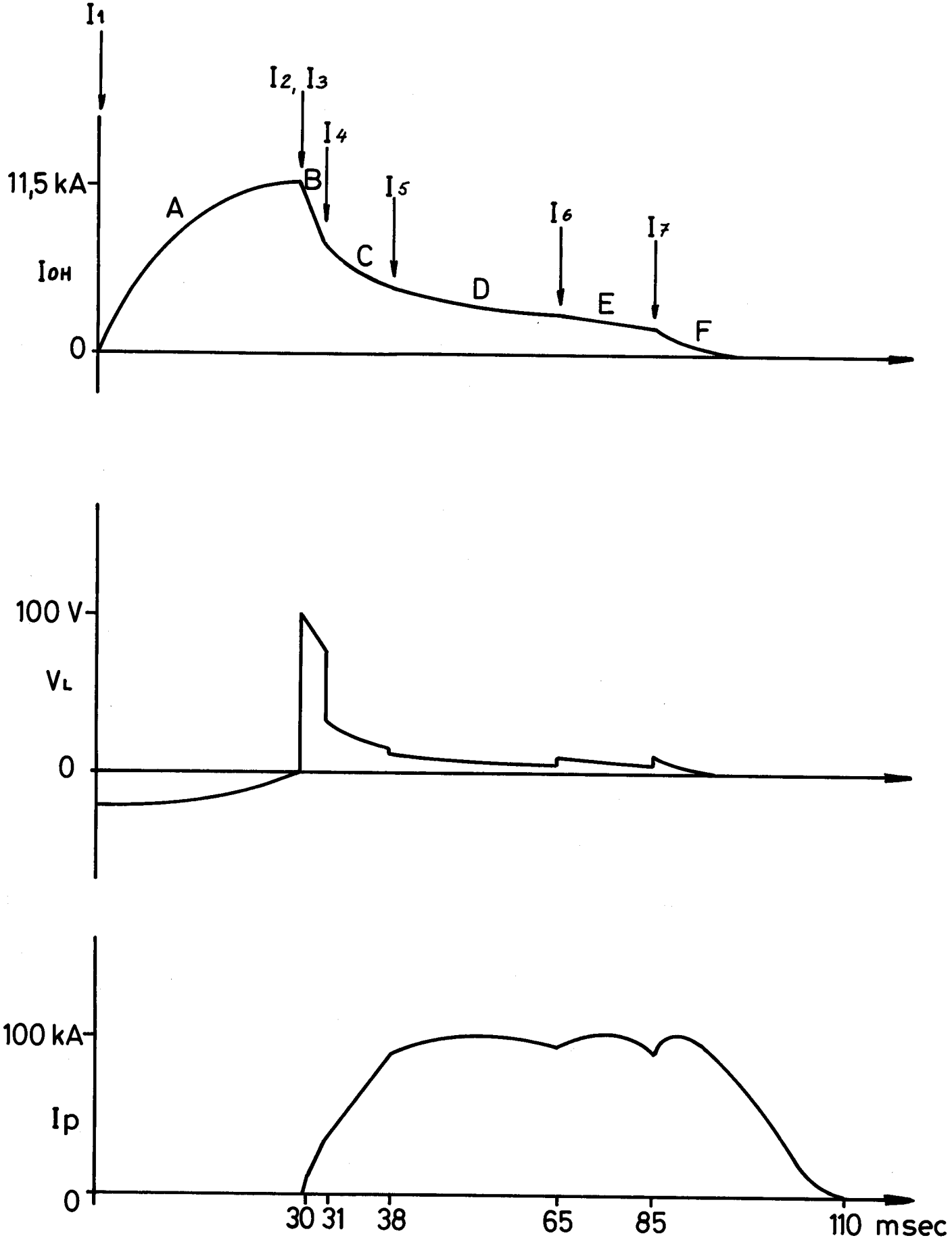

Fig 9 Schematic ohmic heating waveforms

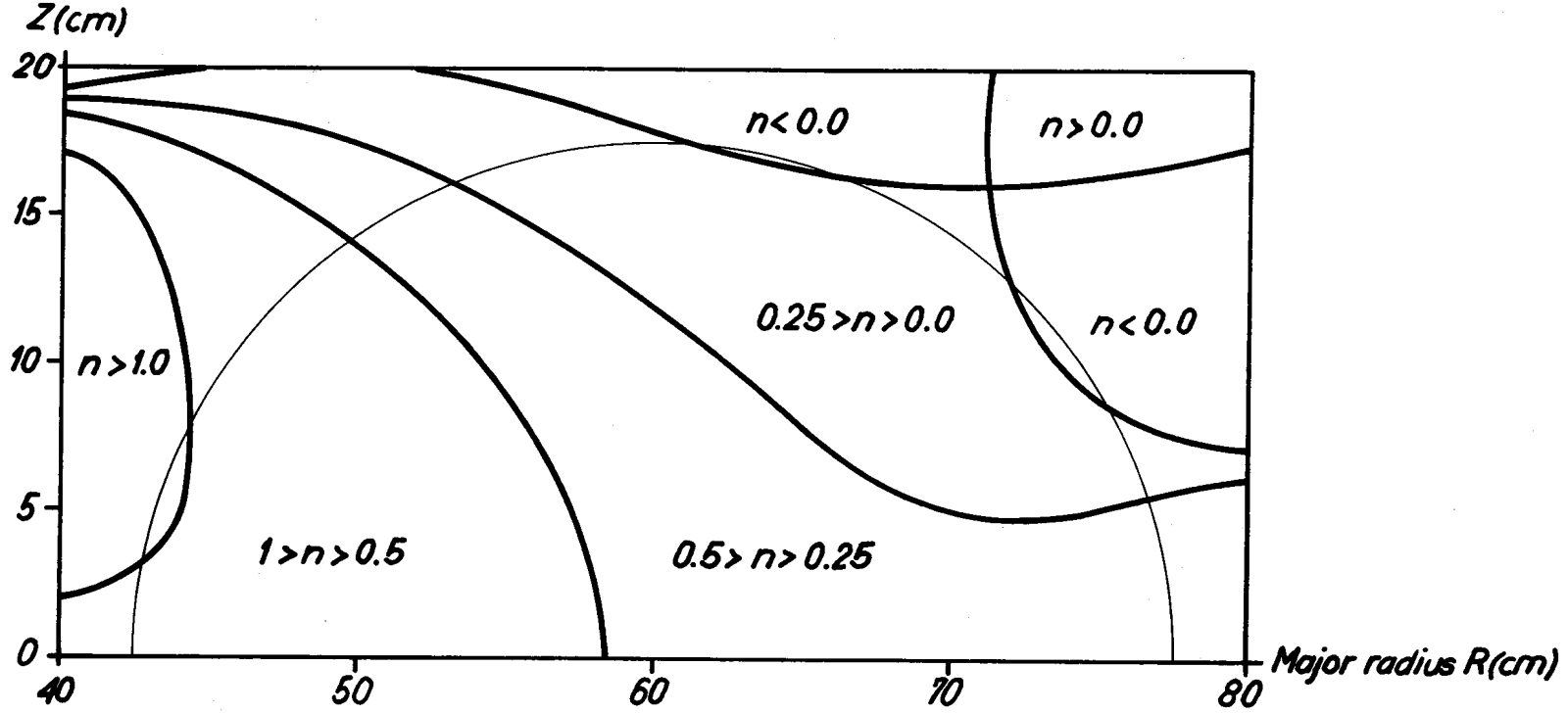

Fig 10 Vertical field curvature index

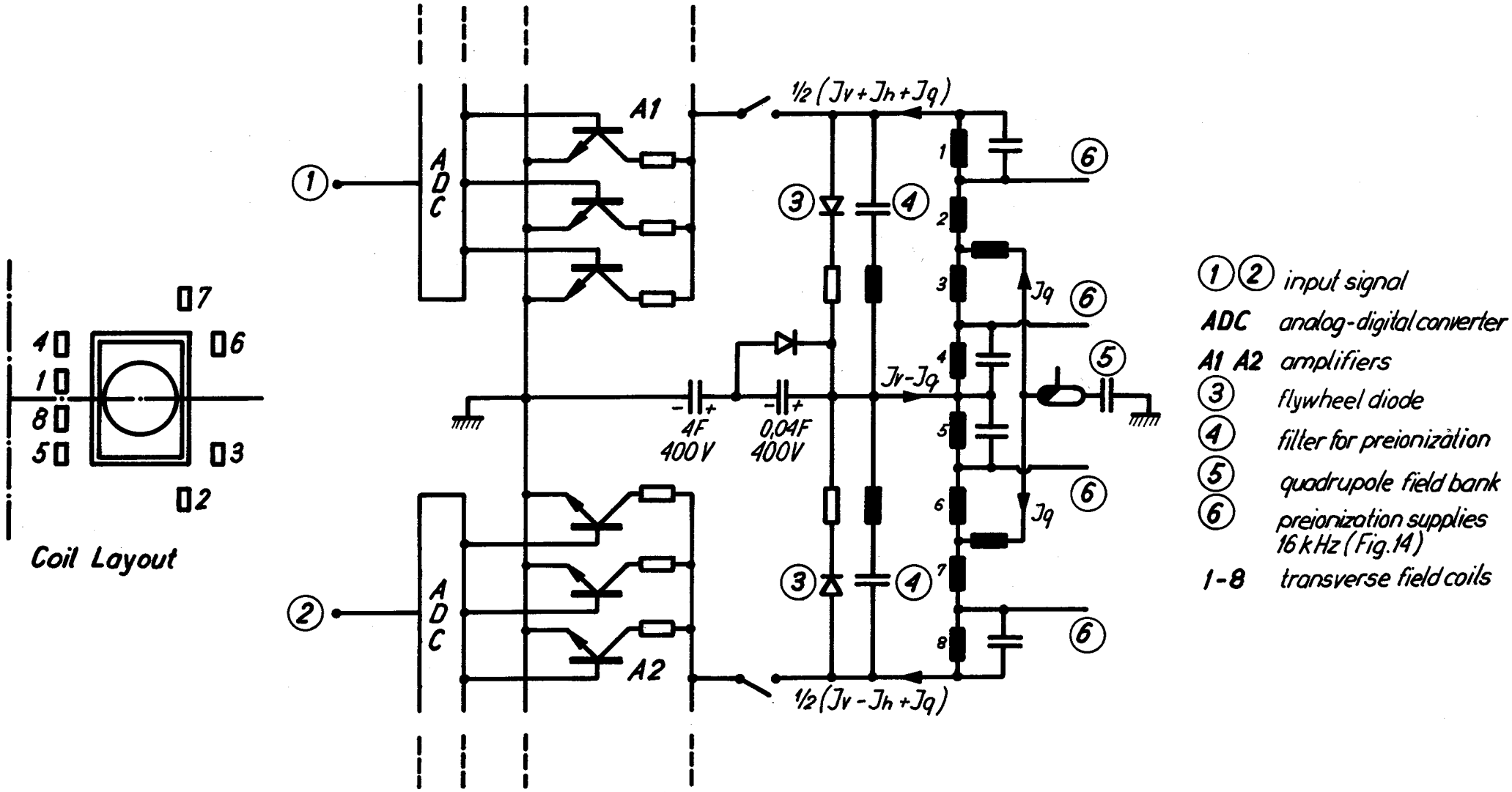

Fig 11 Transverse field power supplies

QUADRUPOLE FIELD POWER SUPPLY

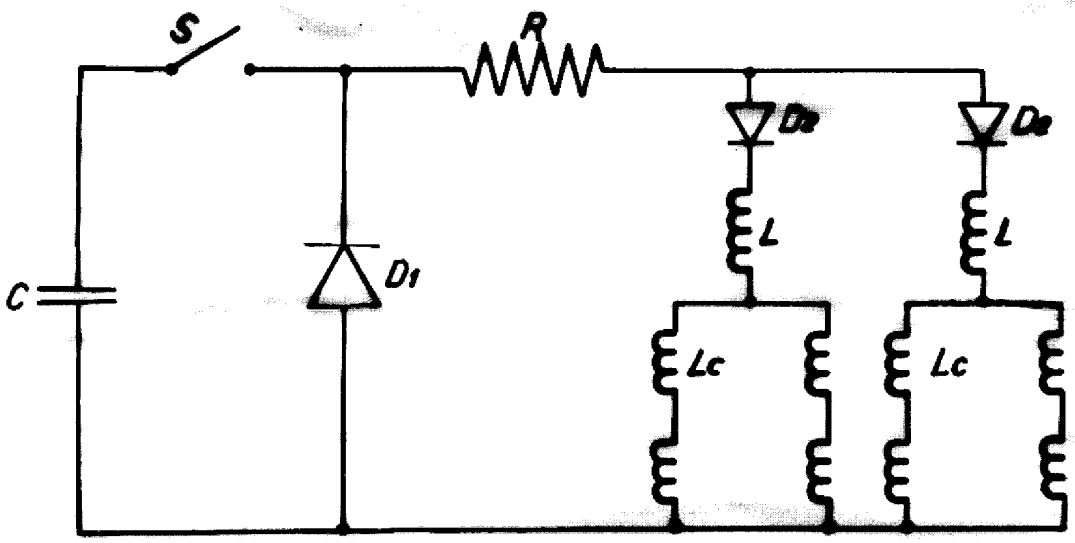

Fig12

C	=	720	μF	Rise Time	=	2.4	msecs.
L	=	12.1	mH	Decay Time	=	3.0	msecs.
L_c	<<	L					
R	=	1.67	Ω	(Includes resistance of Coils)			
D_1	=	Diode clamp.					
D_2	=	Isolation diodes.					
S	=	EE BK7703	Ignition.				

Peak Current I. = 1200 Amps for charging Voltage V_o = 4.8 kV

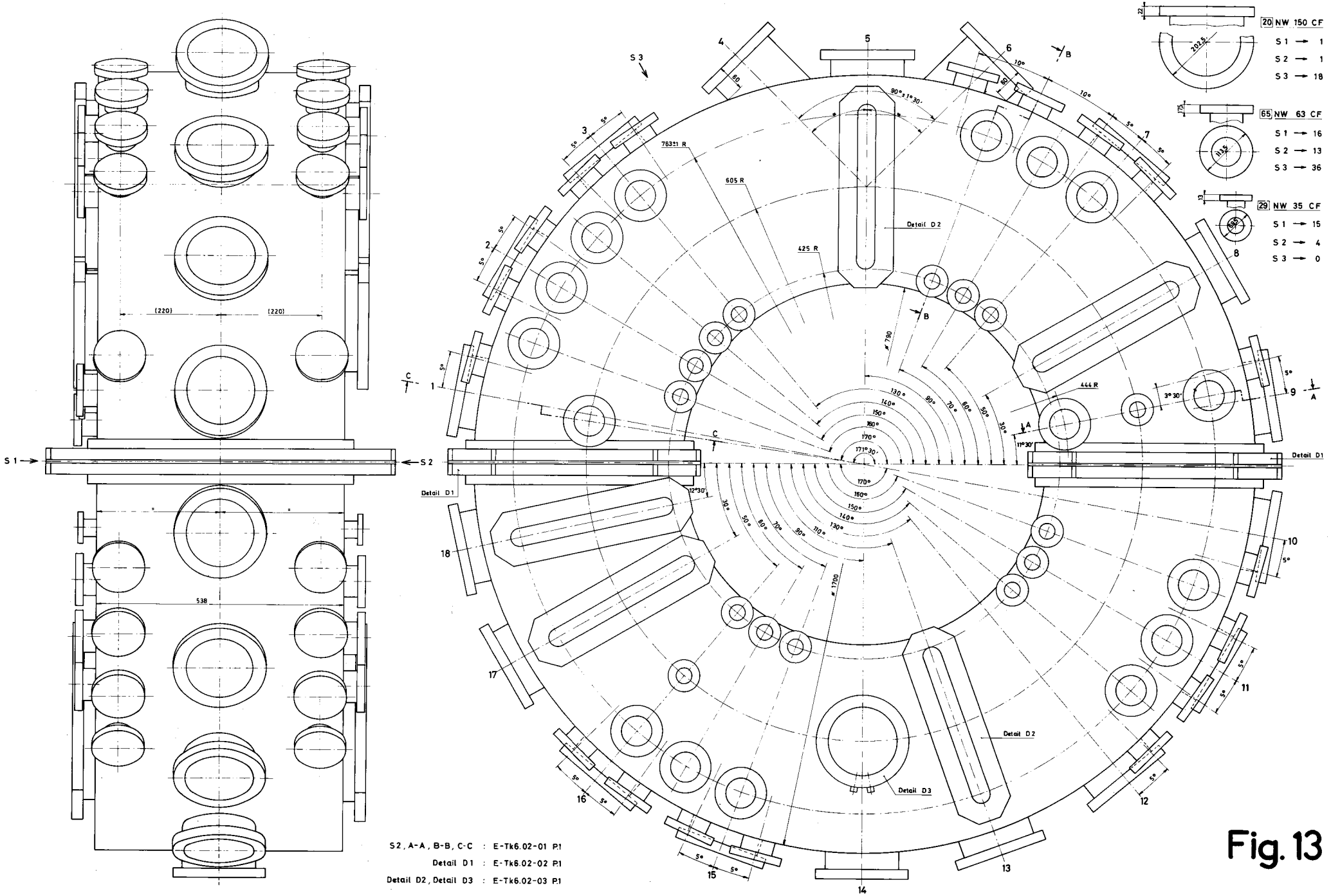

S 2, A-A, B-B, C-C : E-Tk6.02-01 P.1
Detail D 1 : E-Tk6.02-02 P.1
Detail D 2, Detail D 3 : E-Tk6.02-03 P.1

Fig. 13

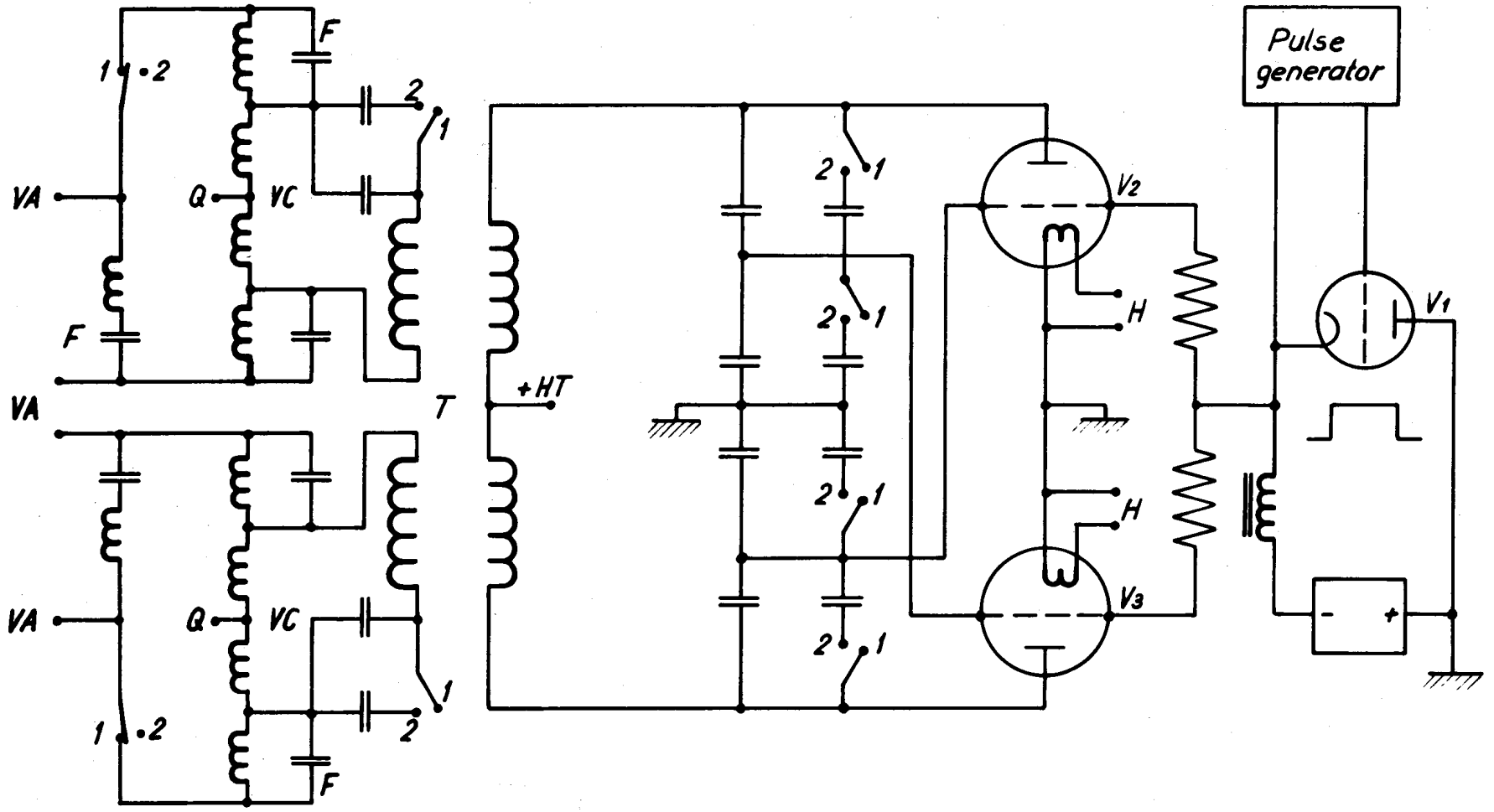

T output transformer
VC vertical field coils
F 16 KHz filters

V_1 grid modulator
V_2, V_3 ITL 30-1 oscillator
H filament heating

Q input of the quadrupole field current
VA to the vertical field generator

Fig. 14 5-16 KHz, 100 KW, Pulsed oscillator
(Pos. 1 - Preionisation; Pos. 2 - Cleaning)

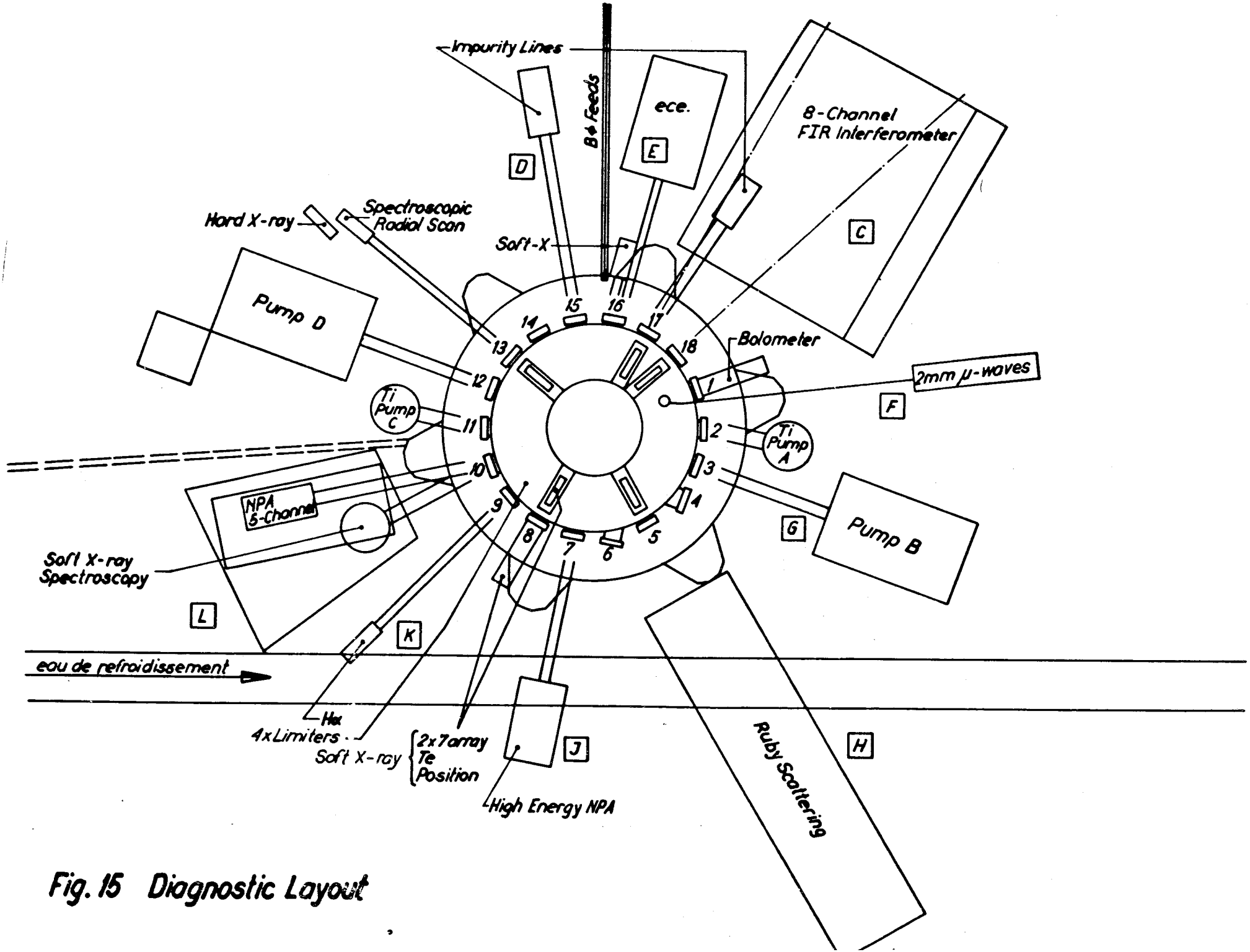

Fig. 15 Diagnostic Layout

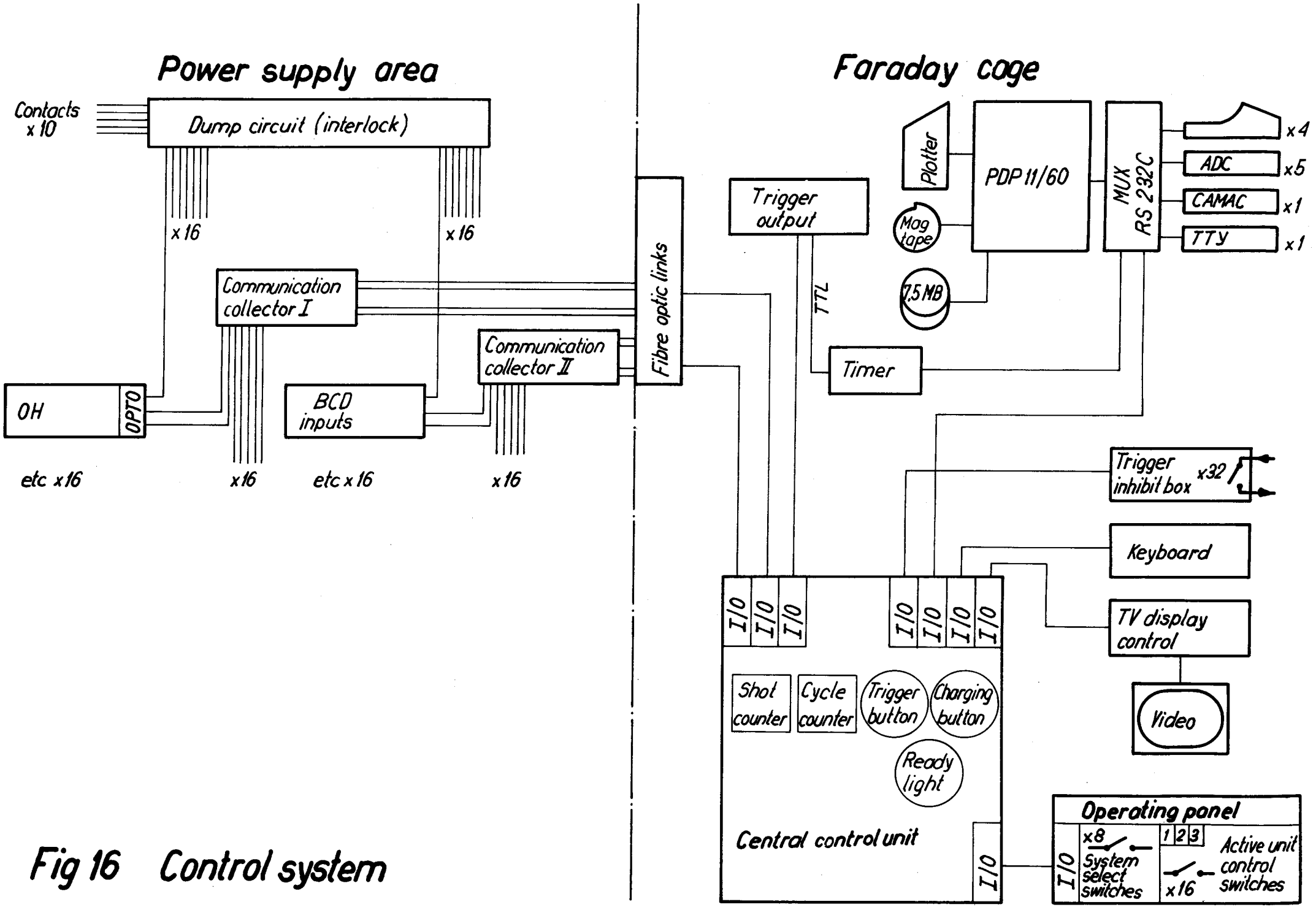

Fig 16 Control system